Russian Geology and Geophysics © 2020, V.S. Sobolev IGM, Siberian Branch of the RAS
Vol. 61, No. 11, pp. 1313–1319, 2020 DOI:10.15372/RGG2019181 *Geologiya i Geofizika*

Influence of "Geologic Noise" on Magnetotelluric–Sounding Data and Methods for Taking It into Account

A.V. Pospeev[a,b,✉], E.A. Sen'[a,c]

[a]*Institute of the Earth's Crust, Siberian Branch of the Russian Academy of Sciences, ul. Lermontova 128, Irkutsk, 664033, Russia*

[b]*Irkutsk Scientific Center, Siberian Branch of the Russian Academy of Sciences, ul. Lermontova 134, Irkutsk, 664033, Russia*

[c]*OOO SIGMA-GEO, ul. Zvezdinskaya 6, Irkutsk, 664011, Russia*

Received 24 January 2019; received in revised form 8 November 2019; accepted 27 November 2019

Abstract—The paper deals with the problem of interpreting magnetotelluric data in the differentiated low-conductivity upper part of the section. An observation network often makes it impossible to describe a spatial irregularity spectrum completely, so, using 3D data inversion comes across a significant spatial equivalence of the solution. The effect of irregular conductivity of the upper part of the section at one of the sites is considered by the comprehensively studied near-field transient electromagnetic sounding in dense 3D networks. A technique is proposed for choosing the directions of the minimum gradient of anomaly-causing conductivity and for selecting corresponding quasi-longitudinal curves for estimating the deeper parameters of the model. The advantage of using quasi-longitudinal curves is shown, and the high geological efficiency of the developed technique for interpreting magnetotelluric data is demonstrated at one of the sites of the Siberian Platform.

Keywords: magnetotelluric sounding; induction and galvanic effects; impedance; conductivity; interpretation; quasi-longitudinal curve

INTRODUCTION

Despite the fact that many publications have been devoted to methods for interpreting magnetotelluric sounding (MTS) data, there has been no successful interpretation algorithms allowing one to obtain the most reliable geological information in any geological conditions. This is explained by the rather complex nature of the effect of nonhorizontal elements of the geoelectric section on the structure of the Earth's magnetotelluric field. At the same time, nonhorizontal effects are additive, so separating the influence of different-level inhomogeneities is also a problem.

From a theoretical point of view, one can recover the geoelectric section under study by using inversion procedures corresponding to the dimensions of the medium. However, 3D inversion procedures that take into account the dimensions of the medium are extremely time consuming. Moreover, the irregularity of observation networks induces spatial equivalence effects. This predetermines the possibility of applying simplified interpretation techniques with reduced inversion dimensions. In practice, in most cases, the upper part of the section is characterized by a very significant geoelectric contrast of objects. Due to the influence of various exogenous processes, it is often highly differentiated geoelectrically and is a strong anomaly-causing object.

STATE OF THE PROBLEM

It is shown by model calculations (Dmitriev et al., 1975) that all types of nonhorizontal inhomogeneity effects on MTS curves are divided into two classes: induction and galvanic. The former are associated with both vertical and lateral propagation of the electromagnetic field in which the flow of magnetotelluric current is longitudinal relative to two-dimensional structures. The latter are due to the formation of an excessive or insufficient amount of charges in the inhomogeneous part of the section during transverse excitation of geoelectric objects.

Galvanic effects are the main factor complicating the behavior of MTS curves (Berdichevskii and Zhdanov, 1981). Due to the lack or excess of charges in an inhomogeneous layer, the right branches of the curves experience a static shift along the ordinate axis. For purely two-dimensional structures, the ratio of the apparent resistance of the transverse and locally homogeneous curves is described by the simple equation

$$\rho^{\perp} = \rho_{1D}\left(\frac{s_i}{s_e}\right)^{\alpha} = \rho_{1D}\cdot K_{gs}, \qquad (1)$$

✉ Corresponding author.
E-mail address: avp@crust.irk.ru (A.V. Pospeev)

where $\rho^{\perp}$ is the resistance of the transverse curve in the range of influence of the galvanic effect, ρ_{1D} is the resistance of the curve locally corresponding to a one-dimensional section, S_i and S_e are the conductivity within the inhomogeneity and the integral conductivity outside of the inhomogeneity, α is the power coefficient approximately equal to the angle of arctangent of the angle of slope of the ascending asymptote of the MTS curve (Dmitriev et al., 1975), and K_{gs} is the galvanic shielding.

ESTIMATED MODELING METHOD

A smoothed conductivity S_e in Eq. (1) can be written as a convolution of the layer conductivity value and the "galvanic" filter coefficients:

$$S_e = f_i \cdot S_j .$$

Here f_i denotes the spatial feature of the filter, and S_j is the conductivity distribution. The former depends on how deep the heterogeneity is located and the "stiffness" of the underlying geoelectric shield. Figure 1 shows the pulse characteristics of the "galvanic" filter for the leftmost block of the model, illustrated in Fig. 4*a*, with the location of inhomogeneities in the above-screen thickness and between the nonconductive screen and the foundation.

In the case of near-surface inhomogeneity, the filter is relatively narrow, which is explained by the sufficient possible "leakage" of transverse currents. The shape of the filter in the case where the inhomogeneity is located between the screen and the foundation also depends on the "stiffness" of the high-resistance screen. The larger the product of the longitudinal conductivity of the above-screen thickness with the transverse resistance of the screen, the wider the transient response of the filter.

The spatial filtering principle is extended to the three-dimensional case. For this purpose, a 3D filter in the central section is formed, similar to a two-dimensional one and attenuating along the *Y* axis in directions from the center. This filter is used to determine the galvanic shielding coefficient K_{gs} as a convolution of S_i/S_e ratios for each *Y*-section of the filter with a Gaussian-like curve. As the galvanic shielding coefficient depends on the direction of field polarization, it is calculated for each reference point as a function of the field direction angle φ.

Based on the principle described above, a program is formed for estimating the azimuthal distribution of the galvanic shielding coefficient.

Direct calculations are carried out using data on the distribution of the oversalt conductivity S_1 of one of the sites within the Angara-Lena Step in the south of the Siberian Platform, studied by the near-field transient electromagnetic sounding (TES) in dense 3D networks. The geoelectric section of the area under study contains three geoelectric complexes of the sedimentary cover, which lie on a high-resistivity crystalline foundation (Fig. 2). The total thickness of the sediments is about 3 km, and their integral conductivity is 30–40 S. The longitudinal resistance of the complexes varies from the first tens to the first hundreds of Ohm·m. It should be noted that the salt interlayers occurring in the middle (carbonate-halogen) complex, have a specific electrical resistance of many tens of thousands of Ohm·m. Because of this, the transverse resistance of the middle complex is extremely high, reaching $(5–10)\cdot 10^7$ Ohm·m^2.

The spatial distribution of S_1 in the indicated area has a complex three-dimensional character, which is related to variations in the geological characteristics of the oversalt complex, namely the influence of fault tectonics, changes in the hydrogeological setting, etc.

For each reference point, the known values of the oversalt conductivity S_1 are used by the program to estimate the galvanic shielding coefficient with the filter turning in the direction every 22.5º. The resulting azimuthal diagrams K_{gs} are combined with the unit circle (Fig. 3).

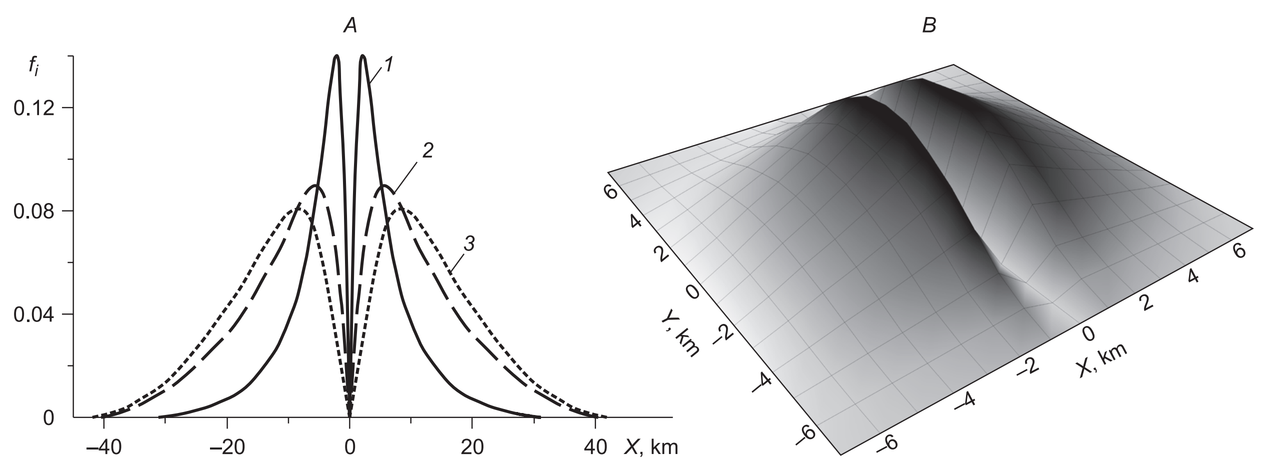

Fig. 1. Filter shape for the formation of S_e: two- (*A*) and three-dimensional (*B*) versions. *1–3*, the shape of the two-dimensional filter with the following position of the inhomogeneity: *1*, above the screen, *2*, below the screen with moderate transverse resistance (< $1\cdot 10^7$ Ohm·m^2), *3*, below the screen with high transverse resistance (>$10\cdot 10^7$ Ohm·m^2).

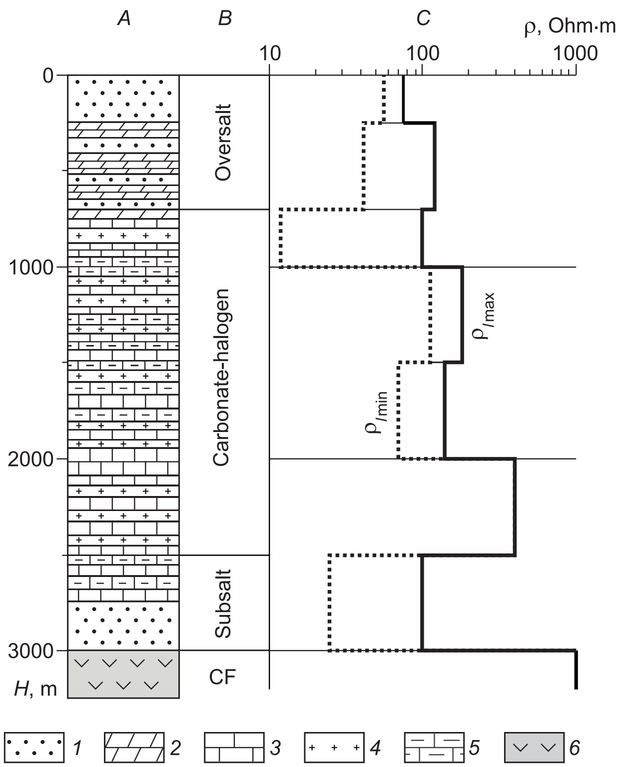

Fig. 2. Geological (*A* and *B*) and geoelectric (*C*) models of the area under study. *1*, sandstones; *2*, marls; *3*, limestones and dolomites; *4*, salts; *5*, mudstones and siltstones; *6*, crystalline rocks of the basement; Ф, crystalline basement, $\rho_{l\,\min}$ and $\rho_{l\,\max}$ denote the approximate minimum and maximum longitudinal resistances of the horizons.

It is shown by analyzing the calculation results, that the nature of distribution of the azimuthal diagrams K_{gs} is complex, depending on the oversalt conductivity anomalies. Thus, within the elongated conducting anomalies, K_{gs} approaches 1 in the longitudinal direction. Within the nonconducting sites, the maximum values of K_{gs} are oriented across the strike of the anomalies, with the minimum components being the least screened. There is a sufficient number of points on the area, within which K_{gs} in all directions is smaller or larger than 1. It can also be noted that, at a certain part of the reference points, the curves of the azimuthal distribution K_{gs} deviate noticeably from an elliptical shape.

Due to the superposition principle, in the presence of several levels of inhomogeneities, the effects of galvanic shielding are summed up.

SPATIAL FEATURES OF INHOMOGENEITIES

In practice, most often the exact parameter distribution of inhomogeneities with a predominant galvanic effect on the MTS curves is unknown, in which case it is impossible to estimate the real relationship between the level of transverse and locally one-dimensional curves.

Having the programs for two-dimensional and three-dimensional modeling does not always ensure that one can obtain geoelectric sections, which are as close as possible to the real conditions of the region under study. This is due not only to the objective limitations of the interpretation device, but also to the obvious influence of the existing lack of necessary information on the reliability of structures.

First of all, this can be explained by the fact that magnetotelluric observation networks usually do not allow one to describe the entire spatial spectrum of inhomogeneities. This problem is especially relevant for inhomogeneities located in the upper part of the section (UPS). Here, due to the significant influence of exogenous processes, media with a

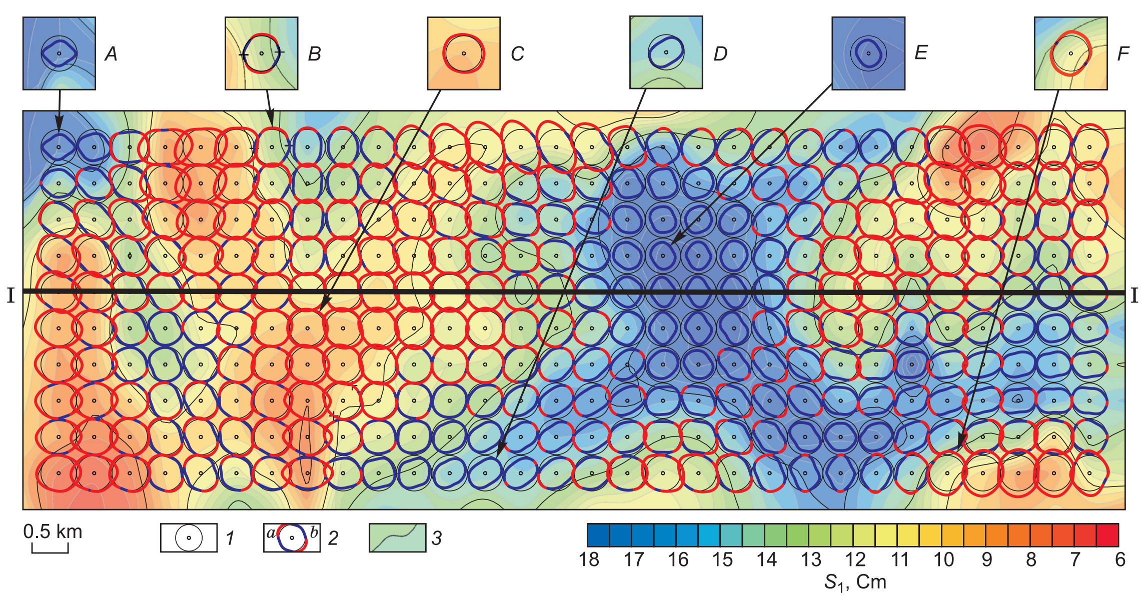

Fig. 3. Calculation results for the azimuthal distribution K_{gs}. *1*, MTS reference points and the unit circle; *2*, azimuthal diagrams K_{gs}: *a*, $K_{gs} > 1$, *b*, $K_{gs} < 1$; *3*, conductivity isolines. The inset above: *A*, complex-shaped azimuthal diagrams; *B*, the effective curve is not deflected in level; *C*, all curves are above the normal level; *D*, the maximum curve is not deflected; *E*, all curves are below the normal level; *F*, the minimum curve is not deflected.

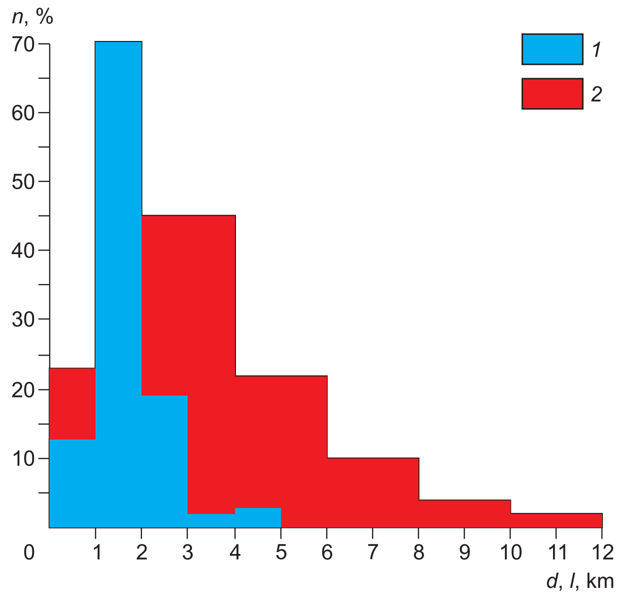

Fig. 4. Distribution histograms of the width (*1*) and length (*2*) of geoelectric anomalies of the oversalt geoelectric complex on the eastern slope of the Nepskii dome.

high contrast of geoelectric properties are formed. Unlike the signal recording process in a time domain, this is the case where systems for suppressing the frequency substitution effect in the form of prefiltering cannot be implemented.

On the other hand, the inhomogeneities of the UPS are rarely an independent object of study in magnetotelluric research. Therefore, the main task of an interpreter is to adequately take into account their influence on MTS curves in order to obtain the most reliable information about the behavior of those parts of the section that are of exploratory interest (Zinger, 1992).

The statistical characteristics of real geoelectric inhomogeneities are estimated by analyzing the spatial conductivity parameters of oversalt, carbonate-halogen, and subsalt complexes in the areas located in the central part of the Nepa-Botuoba anteclise, studied by the TES in dense 3D networks. A step between the points is 400–600 m, which ensures the investigation of anomalous objects larger than one kilometer. The distribution histograms of the width and length of the anomalies are shown in Fig. 4.

As can be seen from the figure, the average size of the anomaly is about 1.5 km. The ratio of the average size of the long and short axes of the anomalies is approximately 2/1. Thus, with the use of a standard 2-km step between MTS points, approximately 70% of the anomalies are missed.

SUBSTANTIATING OF THE INTERPRETATION METHOD

The possible influence of inhomogeneity parameters on the MTS curves is estimated using a 2D modeling program developed by I.L. Vardanyants (1978), and, for the model illustrated in Fig. 5*A*, E- and H-polarization curves are determined.

A

h \ l	3	3	3	3	3	3	3	3	3	3	3	3	3	3	3	3	3	3	3	3	3	3	3	3	3	3	3	3	3	3
0.2	K	K	K	K	K	K	K	K	K	K	K	K	K	K	K	K	K	K	K	K	K	K	K	K	K	K	K	K	K	K
0.5	G	M	H	J	H	J	K	B	K	L	H	F	F	K	K	G	E	E	K	I	E	E	A	D	F	B	G	H	B	K
0.4	K	K	K	K	K	K	K	K	K	K	K	K	K	K	K	K	K	K	K	K	K	K	K	K	K	K	K	K	K	K
0.9	Q	Q	Q	Q	Q	Q	Q	Q	Q	Q	Q	Q	Q	Q	Q	Q	Q	Q	Q	Q	Q	Q	Q	Q	Q	Q	Q	Q	Q	Q
0.9	G	G	G	G	G	G	G	G	G	G	G	G	G	G	G	G	G	G	G	G	G	G	G	G	G	G	G	G	G	G
16	P	P	P	P	P	P	P	P	P	P	P	P	P	P	P	P	P	P	P	P	P	P	P	P	P	P	P	P	P	P
22	N	N	N	N	N	N	N	N	N	N	N	N	N	N	N	N	N	N	N	N	N	N	N	N	N	N	N	N	N	N
105	O	O	O	O	O	O	O	O	O	O	O	O	O	O	O	O	O	O	O	O	O	O	O	O	O	O	O	O	O	O
∞	C	C	C	C	C	C	C	C	C	C	C	C	C	C	C	C	C	C	C	C	C	C	C	C	C	C	C	C	C	C

B

h \ l	3	3	3	3	3	3	3	3	3	3	3	3	3	3	3	3	3	3	3	3	3	3	3	3	3	3	3	3	3	3
0.2	K	K	K	K	K	K	K	K	K	K	K	K	K	K	K	K	K	K	K	K	K	K	K	K	K	K	K	K	K	K
0.5	M	M	M	H	H	H	B	B	B	H	H	H	K	K	K	E	E	E	I	I	I	A	A	A	B	B	B	B	B	B
0.4	K	K	K	K	K	K	K	K	K	K	K	K	K	K	K	K	K	K	K	K	K	K	K	K	K	K	K	K	K	K
0.9	Q	Q	Q	Q	Q	Q	Q	Q	Q	Q	Q	Q	Q	Q	Q	Q	Q	Q	Q	Q	Q	Q	Q	Q	Q	Q	Q	Q	Q	Q
0.9	G	G	G	G	G	G	G	G	G	G	G	G	G	G	G	G	G	G	G	G	G	G	G	G	G	G	G	G	G	G
16	P	P	P	P	P	P	P	P	P	P	P	P	P	P	P	P	P	P	P	P	P	P	P	P	P	P	P	P	P	P
22	N	N	N	N	N	N	N	N	N	N	N	N	N	N	N	N	N	N	N	N	N	N	N	N	N	N	N	N	N	N
105	O	O	O	O	O	O	O	O	O	O	O	O	O	O	O	O	O	O	O	O	O	O	O	O	O	O	O	O	O	O
∞	C	C	C	C	C	C	C	C	C	C	C	C	C	C	C	C	C	C	C	C	C	C	C	C	C	C	C	C	C	C

C

	ρ, Ohm·m
Q	1000
P	700
O	450
N	170
M	75
L	52
K	45
J	41
I	37
H	33
G	29
F	26
E	23
D	20
C	15
B	13
A	10

Fig. 5. Estimated 2D models: *A*, model with 3-km wide blocks; *B*, model that is three times thinner than model; *C*, legend.

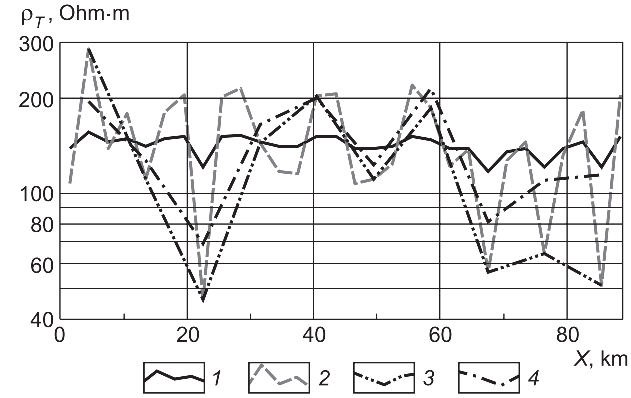

Fig. 6. Charts of ρ_T on a period of 36 s. *1*, one-dimensional curves at reference points; *2–4*, transverse curves for the following models: *2*, *A* with a step of 1 km; *3*, *A* with a step of 3 km; *4*, *B* with a step of 3 km.

This model is formed by inverting the average quasi-longitudinal MTS curve of the south of the Siberian Platform with the addition of inhomogeneities with randomly set parameters into the middle part of the oversalt complex. Figure 5*B* shows the same model, but the width of inhomogeneous blocks is three times larger. Calculation results can be seen in Fig. 6.

It follows from the figure that using the values of the conductivity of the USP, determined at points with a step of 3 km, makes the computational charts of impedances significantly different from thinned ones.

A necessity to suppress the influence of inhomogeneities of the UPS pushes researchers to use methods for accounting for the galvanic bias of the curves. Different approaches may be applied in this case. All of them can be divided into two groups:

– 3D-inversion of full impedance matrices with recovery of the medium parameters at the observation points and between them;

– selection of impedances with subsequent suppression of galvanic influences.

As for the first option, Fig. 6 clearly shows that the solution of a two-dimensional inverse problem using data observed on a network that is more rare than the high-frequency spatial harmonic of inhomogeneities is associated with significant ambiguity. The fact that the observation profile intersects the inhomogeneities in an arbitrary direction can also be a serious complicating factor.

The component selection principle is quite widespread. However, various options for selecting components are used: along the directions of receiving lines (Kaplun, 2014), of mainly maximum lines (Kuz'minykh, 1991), and of minimum lines (Epov et al., 2012).

Let the effectiveness of the selection principle be estimated by analyzing the statistics of inhomogeneities and impedances themselves. Figure 4 shows that the inhomogeneity conductivity is distributed according to a law close to the lognormal law. The geometric parameters of inhomogeneities are distributed in such a way that the number of isometric objects with an axis ratio of 1 : 1–1 : 2 is about 15%, and the number of practically two-dimensional objects with an axis ratio of 1:6 or less is about 30%.

A technique that maximally suppresses the influence may be the selection and interpretation of quasi-longitudinal curves corresponding to those directions along which the ratio of local and external conductivity is closest to unity. The algorithm for selecting quasi-longitudinal curves is quite simple. The role of the first approximation is played by the effective impedance level smoothed in such a way that the influence of "geologic noise" is effectively sup-

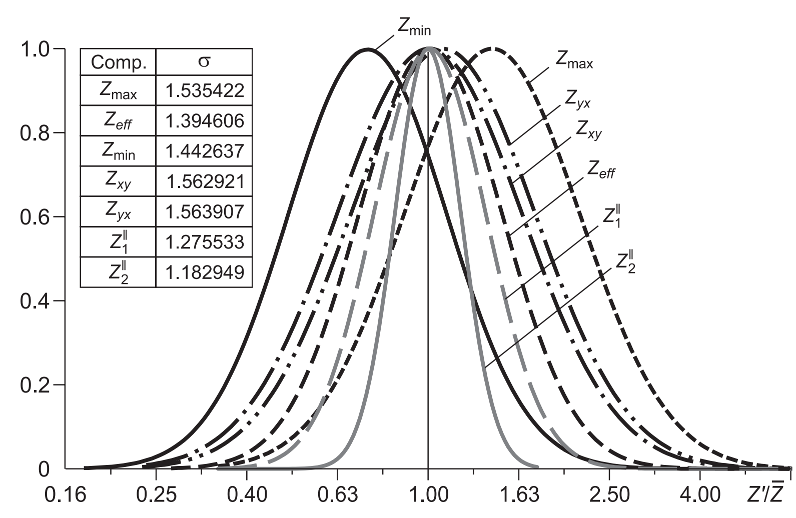

Comp.	σ
Z_{max}	1.535422
Z_{eff}	1.394606
Z_{min}	1.442637
Z_{xy}	1.562921
Z_{yx}	1.563907
$Z_1^{\parallel}$	1.275533
$Z_2^{\parallel}$	1.182949

Fig. 7. Normalized curves approximating the deviation histograms of different impedance components by the normal distribution law at a period of 36 s from an average for the Batholith profile: Z_{max}, maximum; Z_{min}, minimum; Z_{eff}, effective; Z_{xy} and Z_{yx}, along the directions of the receiver; ($Z_1^{\parallel}$), quasi-longitudinal, selected from Z_{max}, Z_{min}, and Z_{eff}; ($Z_2^{\parallel}$), quasi-longitudinal, selected from Z_{max}, Z_{min}, Z_{eff}, Z_{xy}, and Z_{yx}. The table lists the root-mean-square deviations of the components.

pressed, and the influence of the deep part of the section is distorted the least. Then, the components closest to the smoothed effective impedance are selected, and, finally, the final smoothing of the selected quasi-longitudinal components along the profile is performed. The standard deviations of the component ratios to the smoothed effective impedance are shown in Fig. 7. The comparison shows that the use of quasi-longitudinal components significantly reduces the effect of nonzero conductivity gradients. For those selected from Z_{max}, Z_{min}, and Z_{eff} ($Z_1^{\parallel}$), there is a 1.5-fold decrease in the root-mean-square discrepancy as opposed to the effective curves; for those selected from Z_{max}, Z_{min}, Z_{eff}, Z_{xy}, and Z_{yx} ($Z_2^{\parallel}$), there is a twofold decrease.

It is noteworthy that quasi-longitudinal curves have an unbiased estimate. In contrast, the components oriented along the principal axes of the polarization ellipse are characterized by a systematic bias.

The influence of nonzero conductivity gradients along the selected quasi-longitudinal directions can be effectively suppressed using spatial data filtering. In this case, the smoothing parameters are selected in such a way that the deep parts of the section are not unrealistically detailed and that the actually existing deep inhomogeneities are reflected.

Figure 8 shows a seismic-geoelectric section obtained in one of the areas located in the southeast of the Siberian Platform. Here the MTS data for estimating the parameters of the UPS is interpreted using the principles described above. For the formation of the starting model of MTS, the seismic survey materials are used.

The area of work is characterized by a complex geological structure (the presence of large structures of a different order: the Uchur-Maya Plate, the Maya depression, and the Verkhoyansk-Kolyma fold system). The section is represented by terrigenous, terrigenous-carbonate, and carbonate formations of the Riphean, Vendian, and Cambrian, as well as Archean metamorphic rocks.

As a result of the studies, a consistent behavior of geoelectric and reflecting boundaries is observed. It should be noted that the position of the high-resistance geoelectric blocks coincides with the zones of exposition of the crystalline foundation on the day surface: the Ingili stock in the central part and the Nelkan thrust zone in the northeastern part.

There is also a correlation between the change in resistance and the faults of different directions and different orders, identified according to seismic data.

CONCLUSION

The main type of influences causing a bias in the branches of the MTS amplitude curves are galvanic influences associated with the presence of conductivity gradients along the directions of polarization of the magnetotelluric field. Real changes in the conductivity of layers underlain by relatively nonconducting screens form the complex distributions of azimuthal curves of the galvanic shielding coefficient. In more than half of the cases, it is possible to determine such directions along which the conductivity gradient is close to zero and the level of the MTS amplitude curves is not distorted.

In the case where the distribution of the conductivity of the layers underlain by relatively nonconducting screens is complex and unknown, the most effective technique for suppressing galvanic influences is to select quasi-longitudinal curves corresponding to the directions of the minimum conductivity gradients and their additional spatial filtering.

The practical application of this technique for the interpretation of MTS data under various geoelectric conditions has shown its high geological efficiency and good confirmation by further geophysical studies.

The article was written within the framework of the integration project "Fundamental Research and Breakthrough

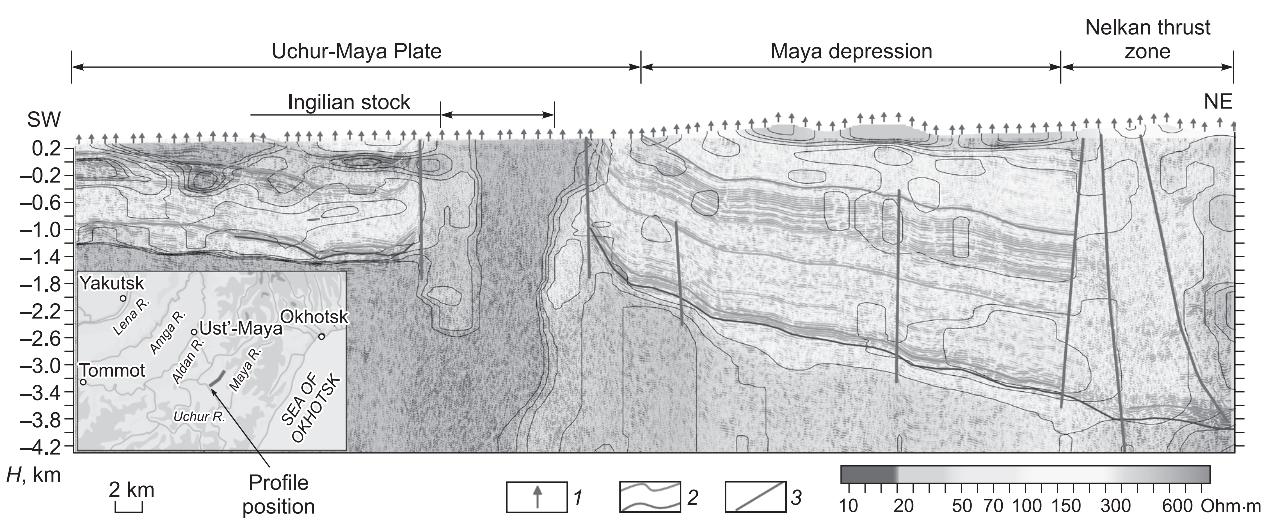

Fig. 8. Seismological section. *1*, MTS points; *2*, reflecting boundaries; *3*, tectonic faults.

Technologies as the Basis for the Advanced Development of the Baikal Region and Its Interregional Ties”.

REFERENCES

Berdichevskii, M.N., Zhdanov, M.S., 1981. Interpretation of Anomalies of the Earth’s Alternating Electromagnetic Field [in Russian]. Nedra, Moscow.

Dmitriev, V.I., Berdichevskii, M.N., Kokotushkin, G.A., 1975. Catalog of Master Charts for Magnetotelluric Sounding in Heterogeneous Media, Part 1 [in Russian]. MGU, Moscow.

Epov, M.I., Pospeeva, E.V., Vitte, L.V., 2012. Crust structure and composition in the southern Siberian craton (influence zone of Baikal rifting), from magnetotelluric data. Russian Geology and Geophysics (Geologiya i Geofizika) 53 (3), 293–306 (380–398).

Kaplun, V.B., 2014. Geoelectric sections of the middle Amur sedimentary basin’s northwestern side based on the data of magnetotelluric sounding. Russ. J. Pass. Geol. 8 (6), 443–455.

Kuz’minykh, Yu.V., 1991. Geoelectric structure of Transbaikalia according to magnetotelluric sounding data, in: Proceeding of IV All-Union Conference on Geomagnetism [in Russian]. Vladimir-Suzdal, pp. 138–139.

Vardanyants, I.L., 1978. Calculation by the grid method of magnetotelluric fields over two-dimensional inhomogeneous media. Part 1. Voprosy Geofiziki, Issue 27, pp. 36–40.

Zinger, B.Sh., 1992. Accounting for statistical distortions in magnetotellurics. Review. Fizika Zemli, No. 5, 53–70.

Editorial responsibility: M.I. Epov